Combining the platinum(II) drug candidate kiteplatin with 1,10-phenanthroline analogues

Benjamin J. Pages,[a] Jennette Sakoff,[b] Jayne Gilbert,[b] Yingjie Zhang,[c] Sharon M. Kelly,[d] James D. Hoeschele,[e] and Janice R. Aldrich-Wright.[*a]

[a] *Nanoscale Organisation and Dynamics Group, Western Sydney University, Campbelltown, NSW 2560, Australia*

[b] *Calvary Mater Newcastle, Waratah, NSW 2298, Australia*

[c] *Australian Nuclear Science and Technology Organisation, Locked Bag 2001, Kirrawee DC, NSW 2232, Australia*

[d] *Institute of Molecular, Cell and Systems Biology, College of Medical, Veterinary and Life Sciences, University of Glasgow, Glasgow, G128QQ, United Kingdom*

[e] *Department of Chemistry, Eastern Michigan University, Ypsilanti, MI 48197, USA*

Abstract

Platinum complexes of the type $[Pt(P_L)(A_L)]^{2+}$ where P_L is a derivative of 1,10-phenanthroline and A_L is *cis*-1,4-diaminocyclohexane (1,4-dach), have been synthesised and characterised by ultraviolet spectroscopy, elemental microanalysis, nuclear magnetic resonance and X-ray crystallography. The calf-thymus DNA binding affinity of these complexes was determined by isothermal titration calorimetry, revealing higher DNA affinity than their 1*S*,2*S*-diaminocyclohexane analogues. *In vitro* cytotoxicity was assessed in ten human cell lines, revealing unexpectedly low activity for the 1,4-dach complexes.

Keywords: platinum, diaminocyclohexane, DNA, cytotoxicity, kiteplatin.

1. Introduction

Cancer is a globally prominent disease in western civilisation; it is the second-highest cause of death and has a lifetime diagnostic rate of 40-50% in Australia and the U.S.A.[1, 2] Chemotherapy remains a widely-used treatment option, and large portion of treatment programs incorporate platinum drugs.[3, 4] The globally approved drugs cisplatin, carboplatin and oxaliplatin are used in these programs; they kill cancerous cells by forming covalent adducts with their DNA.[5] However, these drugs do have drawbacks; treatment results in toxic side effects such as nephrotoxicity, neurotoxicity and myelotoxicity, and there are many cancer types that they are not effective against.[3, 6] These drawbacks have inspired the development of new platinum complexes (PCs) as chemotherapy agents; one example is the complex kiteplatin, which incorporates the ligand *cis*-1,4-diaminocyclohexane (1,4-dach) in the form [Pt(1,4-dach)Cl_2] (Figure 1).[7] Kiteplatin is active against several cell lines that are resistant to cisplatin and oxaliplatin, and is at least as active as oxaliplatin against cells that are sensitive to current agents.[8] Part of the reason for this may be that the 1,2-GG intrastrand adducts formed by kiteplatin inhibit DNA polymerase more than the adducts formed by cisplatin.[9, 10] Research into kiteplatin has recently resurged, with many labs investigating the DNA binding activity of kiteplatin and synthesising platinum(IV) derivatives to improve cytotoxicity.[11-17]

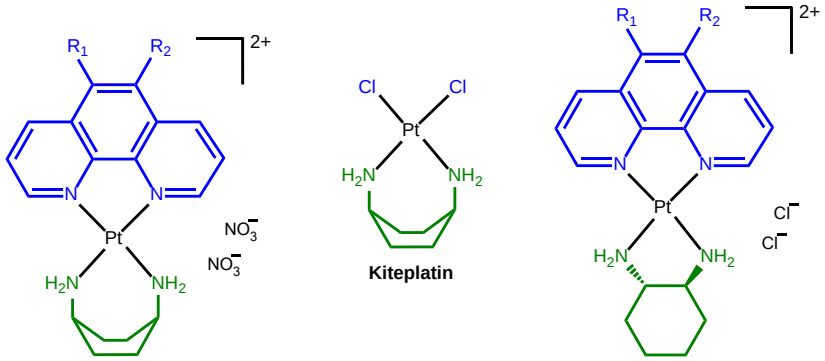

Figure 1. Chemical structures of: 1,4-dach complexes **1-3** (left), 1,2-dach complexes **4-6** (right) and kiteplatin (middle).

Another promising class of PC with potent activity against cisplatin-resistant cells are polyaromatic PCs; these incorporate a polyaromatic ligand (P_L), typically a 1,10-phenanthroline (phen) analogue, and a diamine ancillary ligand (A_L) in the form $[Pt(P_L)(A_L)]^{2+}$. The A_L is usually a 1,2-diaminocyclohexane (1,2-dach) analogue, either 1*S*, 2*S* (*SS*-dach) or 1*R*, 2*R* (*RR*-dach). These PCs are active against cisplatin-resistant cell lines,[18] induce cell death in cancerous cells by a caspase-independent mechanism,[18-20] and bind to DNA through non-covalent intercalation.[21] In particular, the lead complex [Pt(5,6-dimethyl-phen)(*SS*-dach)]Cl_2 (56MESS, Figure 1) is up to 100 times more active than cisplatin in several cell lines, with nanomolar activity against L1210 murine leukaemia and Du145 prostate cancer cells.[21] These polyaromatic PCs and kiteplatin each have demonstrated great potential as platinum drug candidates, due to their different cellular mechanisms and enhanced DNA repair inhibition, respectively, and due to their outperformance of cisplatin in several cell lines. These factors, in addition to kiteplatin's higher activity than that of [Pt(1*R*,2*R*-dach)Cl_2],[8] prompted the development of polyaromatic PCs incorporating 1,4-dach as an A_L and phen, 5-methyl-phen (5Mephen) and 5,6-dimethyl-phen (56Me_2phen) as a P_L (to produce complexes **1, 2** and **3** respectively, Figure 1). Here we present a comparative study between complexes **1**-**3** and their 1,2-dach analogues (including PHENSS, complex **4**, 5MESS, complex **5** and 56MESS, complex **6**, Figure 1) in terms of calf-thymus DNA (CT-DNA) binding by isothermal titration calorimetry (ITC) and *in vitro* cytotoxicity in a panel of human cancer cell lines.

2. Experimental Section

2.1. Materials

[Pt(1,4-dach)Cl_2] (Kiteplatin) was synthesised as per reported previously.[22] All purchased reagents were used as received and all solvents used were of analytical grade or higher. Silver chloride was obtained from BDH chemicals. Dimethyl formamide (DMF) was obtained from Merck. Phen, 5Mephen, 56Me_2phen, dipotassium hydrogen phosphate, potassium dihydrogen phosphate, sodium

chloride and CT-DNA were obtained from Sigma-Aldrich. Methanol was obtained from Chem Supply. Deuterium oxide was obtained from Cambridge Isotope Laboratories.

2.2. Characterisation measurements

NMR spectra were obtained using a 400 MHz Bruker Avance nuclear magnetic resonance spectrometer. All spectra were referenced internally to the deuterium oxide solvent and were obtained at room temperature. ^{1}H spectra were obtained using a spectral width of 15 ppm and 128 accumulations. ^{1}H-^{195}Pt heteronuclear multiple quantum correlation (HMQC) spectra were obtained using a spectral width of 2500 ppm and 256 data points for the ^{195}Pt nucleus (F1 dimension), and a spectral width of 12 ppm and 2048 data points for the ^{1}H nucleus (F2 dimension). The following abbreviations apply to spin multiplicity: s (singlet), bs (broad singlet), d (doublet), dd (doublet of doublets), pt (pseudotriplet), and m (multiplet). The chemical shift (parts per million) of each resonance were quoted as an approximate midpoint of its multiplicity.

Electronic spectra were obtained on a Cary 1E spectrophotometer at a wavelength range of 200-350 nm, using a 10 mm quartz cell. All spectra were recorded at room temperature and were automatically corrected for solvent baseline. Extinction coefficients were obtained through titration of 1 M solution of PC (10 μL) into 2400 μL of water.

Positive-mode electrospray ionisation mass spectrometry (ESIMS) experiments were performed using a Waters TQ-MS triple quadrupole mass spectrometer fitted with an ESI source. Spectra were recorded in positive ion mode from analyte solutions injected (10 μL) into 0.1% trifluoroacetic acid in 50% aqueous acetonitrile flowing at 0.1 mL/min. A capillary voltage of 1.6 kV, cone voltage of 25 V, desolvation temperature of 300 ^{o}C and desolvation flow rate (nitrogen) of 500 L/hr were employed. Spectra were collected over one minute with an *m/z* range of 50-1000.

Microelemental analysis (C, H and N) was performed at the Chemical Analysis Facility, Department of Chemistry and Biomolecular Sciences, Macquarie University. An Elemental Analyser, Model PE2400 CHNS/O produced by PerkinElmer, USA, was used.

2.3. Synthesis of [Pt(P_L)(1,4-dach)]$^{2+}$

Using a modification of a previously established method,[23] kiteplatin (~60 mg, 1 equiv) was dissolved in DMF (~4 mL), silver nitrate (2 equiv) was added and the solution stirred for 16 h at room temperature with light excluded. The resultant silver chloride precipitate was removed by centrifugation. P_L (2 equiv) was added to the supernatant and the solution stirred for 16 h at 50 ^oC, again with light excluded. Another equivalent of P_L was then added and the solution stirred again without light for 16 h at 50 ^oC. The DMF solution was removed through rotary evaporation, the crude product suspended in water and this suspension was filtered. The filtrate was then added to a separatory funnel and washed twice with dichloromethane (20 mL each). The aqueous layer was reduced to a volume of approx. 2.5 mL through rotary evaporation. Purification was achieved through a Sep-Pak® (20 cc, 2 g) column connected to a pump apparatus with UV detector (Bio-Rad, EM-1 Econo™ UV Monitor). The column was activated with methanol (10 mL) and then flushed with water (~40 mL) until the absorbance equilibration. The crude product solution was then loaded onto the column and eluted with water at a flow rate of 1 mL/min. The product was collected, reduced in volume and the Sep-Pak® purification process repeated. Fractions were collected and their contents determined using ^1H NMR. The fractions containing product were combined, reduced under pressure and lyophilised to produce a pale yellow solid. Yield and characterisation data are presented in Table 1, while NMR chemical shifts are presented in Table 2.

Table 1. Summary of the characterisation data of complexes **1-3**.

No	Molecular Formula	Yield (%)	ESI-MS (*m/z*) $[M-H]^+$ Calc.(Found)	Microanalysis Calc.(Found)			UV / λ_{max} (nm) (ε/mol^{-1}.dm^3.cm^{-1}) × 10^2
				C	H	N	
1	[Pt(phen)(1,4-dach)]$(NO_3)_2$·0.25H_2O	70	488.2 (487.8)	34.98 (34.84)	3.67 (3.44)	13.60 (13.53)	278 (280), 226 (345)
2	[Pt(5Mephen)(1,4-dach)]$(NO_3)_2$·1.5H_2O	62	502.2 (501.9)	34.86 (34.96)	4.16 (3.76)	12.84 (12.96)	281 (330), 229 (405)
3	[Pt(56Me_2phen)(1,4-dach)]$(NO_3)_2$·1.5H_2O	71	516.2 (515.8)	35.93 (35.91)	4.37 (3.97)	12.57 (12.59)	285 (340), 231 (450)

Table 2. Summary of the proton and platinum NMR chemical shifts (ppm) of complexes **1-3** and **1′-3′** in D_2O.

Label	**1**	**2**	**3**
H4	8.87 (2H, d, *J* = 8.2 Hz)	8.73 (1H, d, *J* = 8.3 Hz)	8.86 (2H, d, *J* = 8.6 Hz)
H7	-	8.94 (1H, d, *J* = 8.5 Hz)	-
H2	8.72 (2H, d, *J* = 5.5 Hz)	8.63 (1H, d, *J* = 5.6 Hz)	8.61 (2H, d, *J* = 5.4 Hz)
H9	-	8.70 (1H, d, *J* = 5.6 Hz)	-
H5	8.11 (2H, s)	7.86 (1H, s)	-
H3	8.04 (2H, dd, *J* = 8.6, 5.6 Hz)	7.99 (1H, dd, *J* = 8.5, 5.5 Hz)	8.0 (2H, dd, *J* = 8.8, 5.5 Hz)
H8	-	8.06 (1H, dd, *J* = 8.5, 5.5 Hz)	-
CH_3	-	2.78 (3H, s)	2.56 (6H, s)
H1′	3.65 (2H, pt, $^3J_{Pt\text{-}H}$ = 87.0 Hz)	3.65 (2H, pt, $^3J_{Pt\text{-}H}$ = 84.1 Hz)	3.67 (2H, pt, $^3J_{Pt\text{-}H}$ = 76.8 Hz)
HA′	1.90 (4H, m)	1.90 (4H, m)	1.91 (4H, m)
HA′	1.79 (4H, m)	1.78 (4H, m)	1.79 (4H, m)
$^1H/^{195}Pt$	8.83, 2760	8.82, 2690	8.83, 2700

2.4. X-ray crystallography

Single crystals of complex **1** were obtained by dissolving small amounts of sample in hot water and allowing the solution to cool to room temperature. Single crystal data for **1** was collected on the MX1 beamline at the Australian Synchrotron using Si<111> monochromated synchrotron X-ray radiation (λ = 0.71074). Data collection was performed at 100(2) K using BlueIce software[24] and corrected for polarisation and Lorentz effects using XDS software.[25] The absorption correction was then applied to the data using SADABS.[26] The structure was solved with direct methods using SHELXT[27, 28] and full-matrix least-squares refinement was performed using SHELXL-2014[27, 29] via the Olex[2] interface.[30] Two diffractions affected by beam stops were removed in the final structure refinement. All non-hydrogen atoms with occupancies over 0.5 were located from the electron density map and were refined anisotropically. The disordered lattice water molecule was modelled and refined isotropically without added hydrogen atoms, causing a B-level alert in the checkCIF. Hydrogen atoms bound to carbon and nitrogen were added in ideal positions and refined using a riding model. Crystallographic refinement parameters are summarised in Table 3. Supplementary crystallographic data for **1** can be found under CCDC 1583091. This data can be obtained free of charge at http://www.ccdc.cam.ac.uk/conts/retrieving.html, or from the Cambridge Crystallographic Data Centre, 12 Union Road, Cambridge CB2 1EZ, UK; fax: (+44) 1223-336-033; or e-mail: deposit@ccdc.cam.ac.uk.

Table 3. Crystallographic data and structure refinement details for complex **1**.	
Parameters	Values
Empirical formula	$C_{18}H_{22}N_6O_{7.25}Pt$
Formula weight	633.50
Temperature/K	100(2)
Crystal system	monoclinic
Space group	C2/c
a/Å	13.864(3)
b/Å	25.762(5)
c/Å	6.5990(13)
β/°	110.57(3)
Volume/Å^3	2206.7(9)
Z	4
ρ_{calc} /mg mm^{-3}	1.907
μ/mm^{-1}	6.412
F(000)	1232
Crystal size/mm	0.12; 0.03; 0.03
2Θ range for data collection/°	1.581 to 27.499°
Index ranges	$-18 \leq h \leq 18$, $-33 \leq k \leq 33$, $-8 \leq l \leq 8$
Reflections collected	17054
Independent reflections	2471 [R_{int} = 0.0419, R_{sigma} = 0.0211]
Data/restraints/parameters	2469/0/152
Goodness-of-fit on F^2	1.065
Final *R* indexes [$I>=2\sigma(I)$]	R_1 = 0.0380, wR_2 = 0.1066
Final *R* indexes [all data]	R_1 = 0.0384, wR_2 = 0.1070
Largest diff. peak/hole / e Å^{-3}	1.63/-2.24

2.5. Isothermal titration calorimetry – DNA Binding

CT-DNA binding was assessed using a MicroCal ITC 200 calorimeter operating at 37 °C. Each platinum complex (564-750 μM) was titrated into a solution of CT-DNA (160 μM) in K_2HPO_4/KH_2PO_4 (10 mM, pH 7.0) and NaCl (50 mM) buffer. For a baseline, each PC was titrated into buffer alone, and this trace was subtracted from the PC-DNA binding trace. The titration program consisted of one 0.4 μL addition followed by 18 titrations of 2 μL, with a spacing of 180 s, reference power of 6 μcal/s and stirring speed of 750 rpm. Data was analysed using Origin 7.0 (MicroCal version) using 200 iterations of a one-site binding model using the following equations. Experiments were performed in duplicate for each PC.

$$\Delta G = -RT \ln K$$

$$\Delta S = \frac{\Delta H - \Delta G}{T}$$

2.5. In vitro cytotoxicity

Cytotoxicity assays were performed at the Calvary Mater Newcastle Hospital, Waratah, NSW, Australia. The cell lines tested were HT29 colon carcinoma, U87 glioblastoma, MCF-7 breast cancer, A2780 ovarian cancer, H460 lung cancer, A431 skin cancer, Du145 prostate cancer, BE2-C neuroblastoma, SJ-G2 glioblastoma, MIA pancreas cancer, and the non-tumour derived MCF10A breast line. All test agents were prepared as 30 mM stock solutions in water and stored at -20 ºC. All cell lines were cultured in a humidified atmosphere 5% CO_2 at 37 ºC. The cancer cell lines were maintained in Dulbecco's modified Eagle's medium (DMEM) (Trace Biosciences, Australia) supplemented with 10% foetal bovine serum, 10 mM sodium bicarbonate penicillin (100 IU/mL), streptomycin (100 µg/mL), and glutamine (4 mM). The non-cancer MCF10A cell line was cultured in DMEM:F12 (1:1) cell culture media, 5% heat inactivated horse serum, supplemented with penicillin (50 IU/mL), streptomycin (50 µg/mL), 20mM Hepes, L-glutamine (2 mM), epidermal growth factor (20 ng/mL), hydrocortisone (500 ng/mL), cholera toxin (100 ng/mL), and insulin (10 ug/mL).Cytotoxicity was determined by plating cells in duplicate in 100 mL medium at a density of 2,500–4,000 cells per well in 96 well plates. On day 0, (24 h after plating) when the cells were in logarithmic growth, 100 µL medium with or without the test agent was added to each well. After 72 h drug exposure growth inhibitory effects were evaluated using the MTT (3-[4,5-dimethylthiazol-2-yl]-2,5-diphenyl-tetrazolium bromide) assay and absorbance read at 540 nm. An eight point dose response curve was produced from which the IC_{50} value was calculated, representing the drug concentration at which cell growth was inhibited by 50% based on the difference between the optical density values on day 0 and those at the end of drug exposure.

3. Results and Discussion

3.1. Synthesis and characterisation

Synthesis of complexes **1-3** could not be achieved through the typical reflux used for complexes of this type.[31] NMR experiments suggested that much of the 1,4-dach was detached from the platinum centre, with only minor amounts of the final product formed. Instead, a gentler synthesis was undertaken to keep the 1,4-dach ligand coordinated. The addition of silver nitrate in DMF resulted in the conversion of [Pt(1,4-dach)Cl_2] to the intermediate [Pt(1,4-dach)$(DMF)_2$]$(NO_3)_2$; the leaving groups of this product are more labile, allowing the reaction with phen derivatives to take place at 50 ^oC rather than 100 ^oC. The phen addition was slow and incomplete with only one equivalent, and so two equivalents were used instead, with a third added the next day to ensure that as much of the product formed as possible. Scheme 1 summarises the synthesis process.

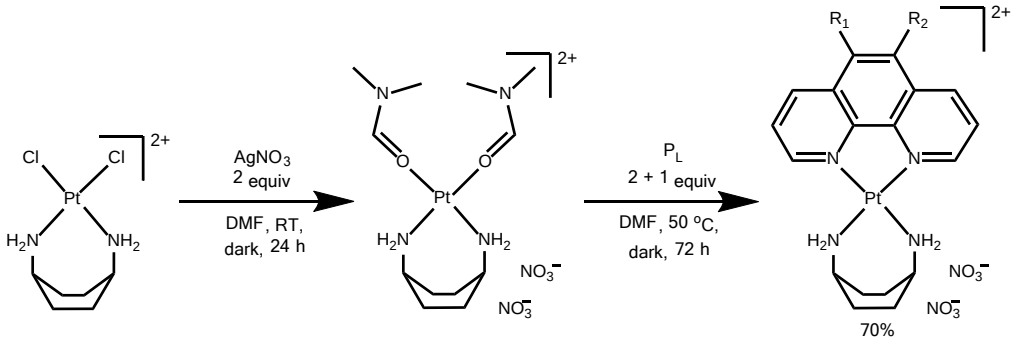

Scheme 1. General synthesis of complexes **1-3**. R_1 and R_2 are either H, CH_3, or a mixture of the two.

The filtering and DCM washes removed most of the excess phen, while the column purification removed the rest. During Sep-Pak® purifications in our previous work, the [Pt(1,2-dach)Cl_2] intermediate typically eluted before the final product, with minor overlap of elution profiles. Here, the elution profile of the [Pt(1,4-dach)$(DMF)_2$]$(NO_3)_2$ intermediate overlapped with the product to a much greater extent. To maximise separation, the flow rate was set to 1 mL min^{-1}, which was the lowest speed achievable without allowing diffusion to occur in the column. Even so, it typically took two runs through the column to separate most of the product from impurities. The gentler

reaction conditions and difficult separation are thought to be the reasons for the relatively low yields of ~70% compared to the typical yields of 80-85% of similar complexes.[32, 33] The identity and purity of these complexes was confirmed through NMR spectra, mass spectra and elemental analysis. The electronic transitions in the UV spectra (Section S1) of **1**-**3** were comparable with those of similar phen platinum(II) analogues;[33] the presence of methyl substituents on the phenanthroline resulted in a red-shift of each peak and the appearance of a shoulder in the peak at approx. 280 nm.

3.2. NMR spectral assignment

Characterisation of all complexes was achieved using ^{1}H NMR and ^{1}H-^{195}Pt heteronuclear multiple quantum correlation (HMQC) NMR. The NMR spectra of complex **3** are shown as an example (Figures 2 and 3). For all complexes, the aromatic region signals of the phen derivatives exhibited the expected chemical shifts and multiplicities as per previous studies.[33] In the aliphatic region, the 1,4-dach signals were similar to that of kiteplatin; the H1′ proton presented a pseudo triplet due to platinum satellites at 3.67 ppm, and the multiplets corresponding to the other aliphatic protons (HA′) were present from approx. 1.95-1.75 ppm. The amine protons were not present due to exchange with D_2O. To confirm the coordination of each ligand to the platinum centre, the ^{1}H-^{195}Pt NMR spectra of all complexes were obtained. These spectra demonstrated a series of proton correlations with a platinum resonance at approx. -2700 ppm. For example, the ^{1}H-^{195}Pt NMR spectrum of complex **3** (Figure 3) revealed a correlation between the phen proton H2 and Pt at 8.72 ppm, as well as between the 1,4-dach proton H1′ and Pt at 3.86 and 3.67 ppm. The Pt chemical shifts of **1**-**3** were slightly higher than those reported for phen complexes of 1,2-dach (approx. -2800 ppm).[34] This kind of platinum peak difference was observed for complexes of 1,2-diaminocyclopentane (approx. -2550 ppm), which was attributed to the ring strain of the pentane.[33] This suggests that a similar phenomenon has occurred here with complexes **1**-**3**, although to a lesser extent, and demonstrates the sensitivity of the platinum nucleus to changes in environment.[35]

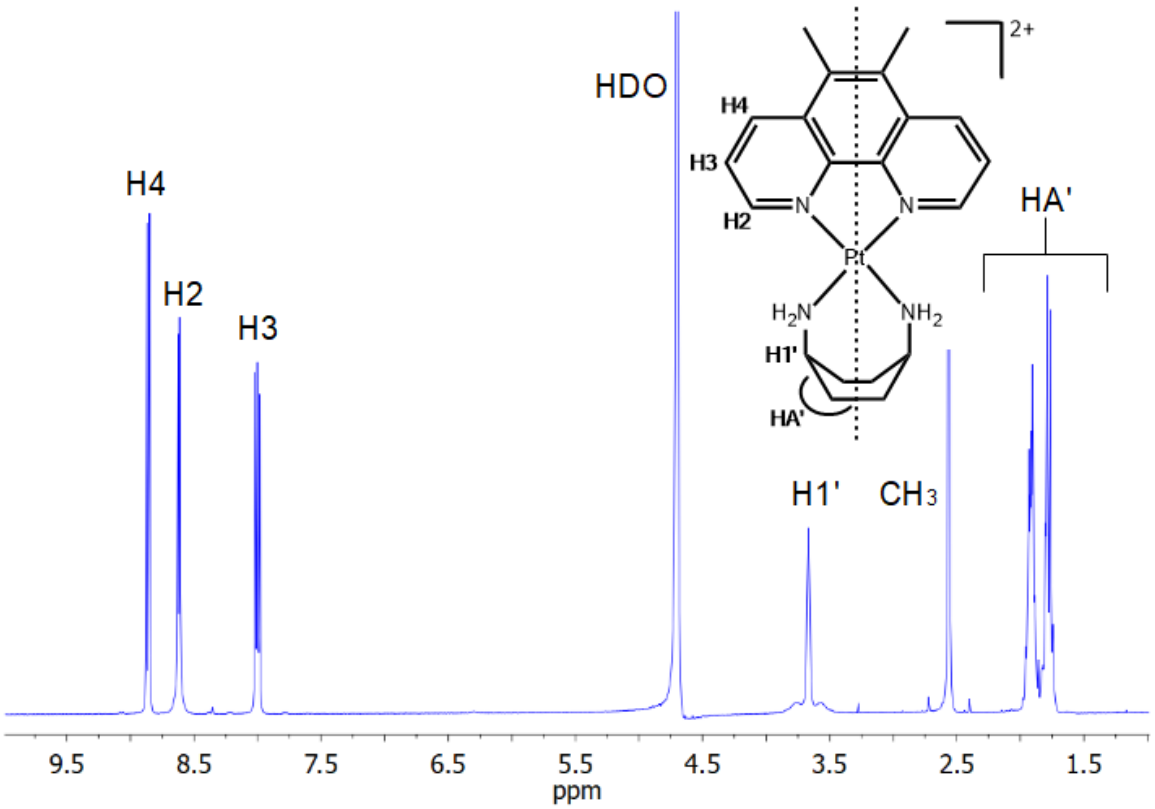

Figure 2. ^{1}H NMR spectrum of complex **3** in D_2O, showing proton assignment. Inset: the structure of **1**, showing proton NMR number assignment. Amine protons are not present due to D_2O exchange.

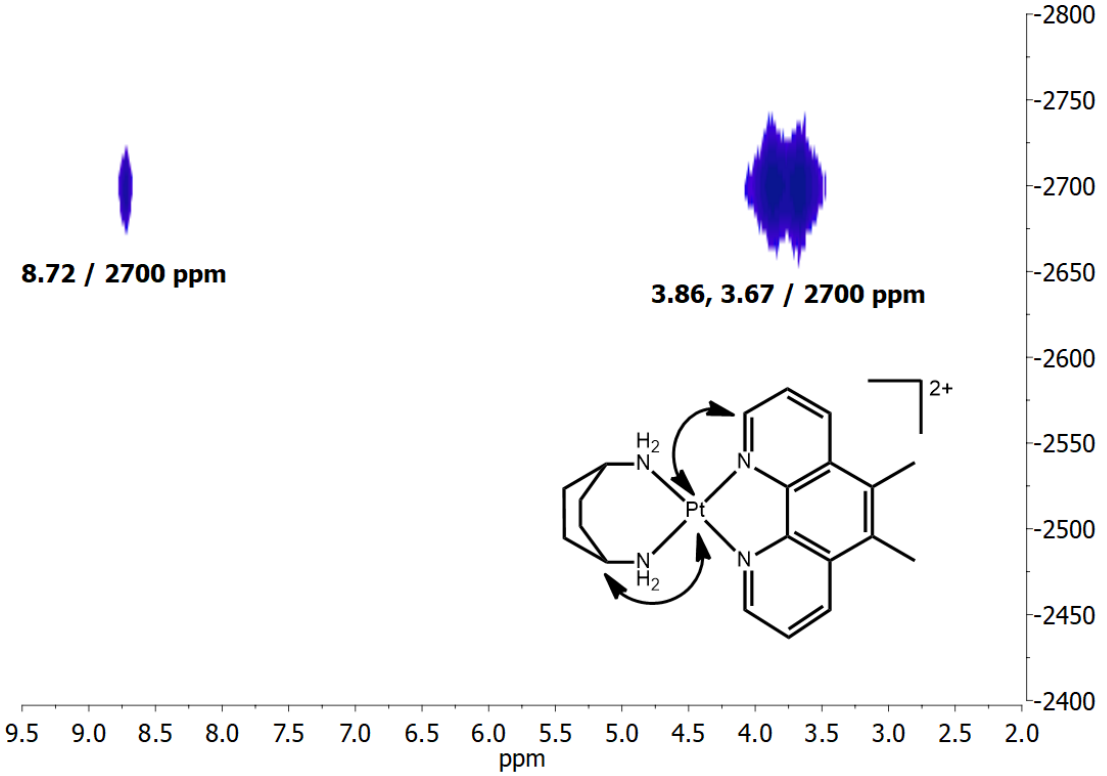

Figure 3. The ^{1}H-^{195}Pt HMQC spectrum of complex **3** in D_2O, showing cross peak assignment of the platinum centre and proton resonances.

*3.3. X-ray crystal structure of complex **1***

The crystal data and structural refinement details are summarised in Table 3 and selected bond lengths, angles and torsion angles are shown in Table 4. The asymmetric unit of **1** contains a half molecule and the full structure is generated by a two-fold symmetry expansion. The complex consists of a PtN_4 coordination sphere with a square-planar coordination geometry for the platinum metal centre (Figure 4). The bond lengths and angles related to the phen ligand and platinum are consistent with the previously published polyaromatic PCs.[32, 33] The 1,4-dach ligand adopted a twist-boat conformation similar to that seen in previous 1,4-dach complexes,[7, 15, 36] with a N2-Pt1-N2 bond angle of 96.3(3)° and Pt1-N2-C7 angle of 125.6(4)°. The N-Pt-N angle is approximately 13° larger than that of previous 1,2-dach complexes that adopt a chair conformation.[32, 33] Relative to complexes of 1,2-dach, the large bite angle of the coordinated 1,4-dach ligand appears to have had no effect on the conformation of the opposing phen ligand. Adjacent phen ligands stack along the *c* axis, with carbon-carbon distances between 3.4-3.5 Å (Fig. 4B). This correlates with π-π interactions.[37]

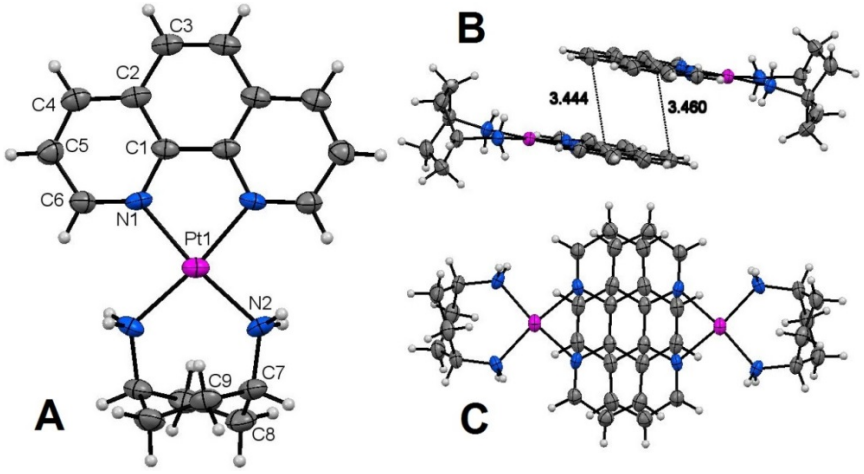

Figure 4. Crystal structure of complex **1**: An ellipsoidal plot (probability 50%) showing the atom numbering system (A) and stacking views from a side (B) and top-down (C). Colour code: Pt in purple, N in blue, C in grey and H in white. Nitrate counter-ions and lattice water molecules have been omitted for clarity. Selected bond lengths (Å): Pt1-N1: 2.062(4), Pt1-N2: 2.072(4). Selected bond angles and torsion angles (°): N1-Pt1-N1: 81.7(2), N1-Pt1-N2: 172.6(2), N2-Pt1-N2: 96.3(3), Pt1-N2-C7: 125.6(4), N1-C1-C1-N1: 0.7(8).

3.4. DNA binding studies

The DNA binding of **1-3** was assessed to determine if there were any differences in affinity between the 1,4-dach complexes and those of *S,S*-dach (complexes **4-6**). **5a**, the nitrate salt of **5**, was also tested to determine if the counter-ion had any effect. The thermodynamic parameters of each PC-DNA interaction are summarised in Table 4, and the ITC trace of **3** is shown as an example (Figure 5). Similar to previous experiments with **6**,[21] the binding of **1-3** with CT-DNA resulted in two peaks per titration rather than one, again suggesting that the binding was biphasic in nature. All binding was spontaneous, with negative changes in enthalpy and overall negative Gibbs free energy. The affinity of **5** was found to be slightly higher than that of **5a**, which suggests that the presence of chloride counter-ions results in a slightly higher DNA affinity than complexes with nitrates. The ΔH and $T\Delta S$ differences between **5** and **5a** are too small to make any meaningful statement regarding thermodynamics, and so reason behind this difference in affinity is unknown. Counter-ions were recently shown to effective DNA affinity to a larger extent for a pair of cobalt complexes,[38] so this phenomenon is not unusual. Regardless, the affinity of complexes **1-3** were found to be ~0.7-2.4 × 10^5 M^{-1} higher than that of their *SS*-dach counterparts (Figure 6). This suggests that the 1,4-dach ligand does impact the DNA binding of these PCs to some extent, and minor changes in DNA binding behaviour based upon A_L have been observed previously.[23] The P_L trend of 56Me_2phen > 5Mephen > phen was observed for **1-3**, although the affinity of **2** relative to **3** was slightly higher than expected.

Table 4. Isothermal titration calorimetry data for complexes **1-6** and **5'**.

No	Complex	10^{-5} K [M^{-1}]	N	ΔH [kcal mol^{-1}]	$T\Delta S$ [kcal mol^{-1}]	ΔG [kcal mol^{-1}]
1[a]	PHENK	2.87 ± 0.04	0.257 ± 0.006	-2.5 ± 0.1	5.2 ± 0.1	-7.7 ± 0.1
2[a]	5KITE	6.2 ± 0.4	0.31 ± 0.01	-3.8 ± 0.1	4.2 ± 0.1	-8.1 ± 0.2
3[a]	56KITE	7.7 ± 0.8	0.325 ± 0.005	-6.0 ± 0.1	2.1 ± 0.2	-8.1 ± 0.2
4[b,c]	PHENSS	2.0 ± 0.3	0.27 ± 0.01	-3.7 ± 0.1	3.9 ± 0.4	-7.5 ± 0.7
5[b]	5MESS	3.8 ± 0.2	0.271 ± 0.004	-3.5 ± 0.2	4.3 ± 0.1	-7.8 ± 0.2
6[b,c]	56MESS	5.7 ± 0.5	0.33 ± 0.01	-5.6 ± 0.1	2.6 ± 0.2	-8.2 ± 0.6
5a[a]	5MESS	3.2 ± 0.3	0.265 ± 0.004	-3.4 ± 0.1	4.3 ± 0.1	-7.7 ± 0.2

a – tested as a nitrate salt, b – tested as a chloride salt, c – values from reference [21].

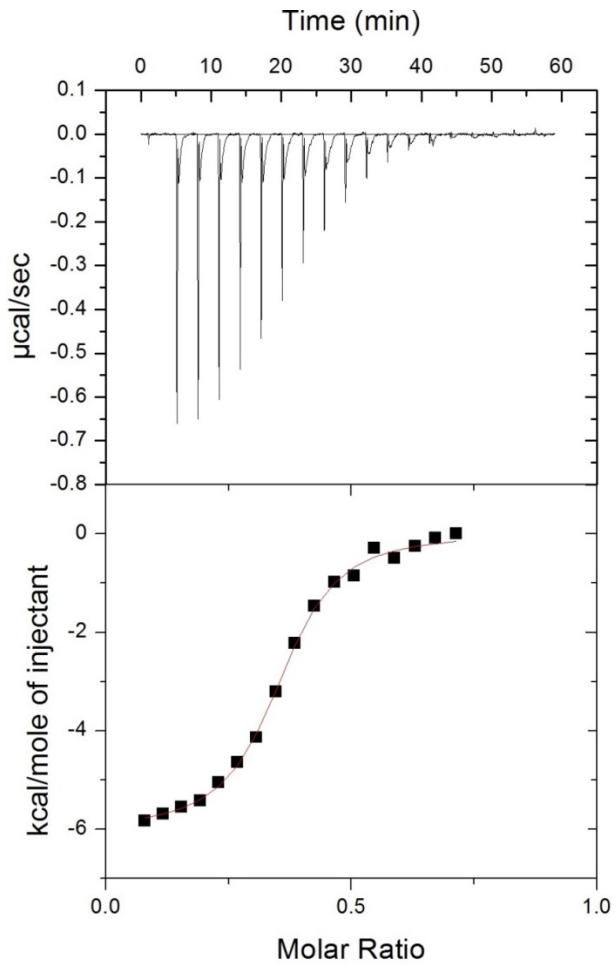

Figure 5. ITC trace and binding curve of the titration of complex **3** (564 µM) into CT-DNA (160 µM). Fits were obtained using a one-site binding model.

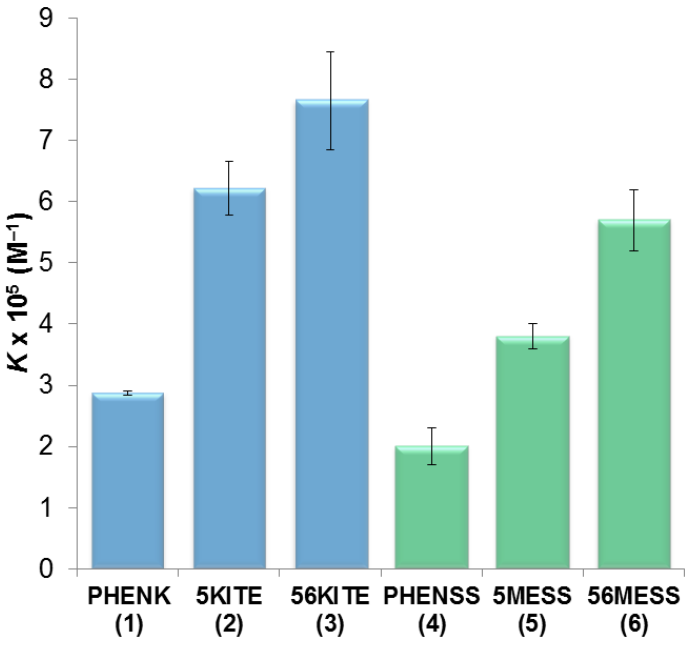

Figure 6. Comparison of the DNA binding constants of **1**-**3** (1,4-dach, blue) and **4**-**6** (*SS*-dach, green).

3.5. In vitro *cytotoxicity*

The *in vitro* cytotoxicity of complexes **1-3** was assessed using the MTT assay in ten human cancer cell lines and one "normal" cell line. These data were compared with those of **4-6** and their *R,R* isomers (**4'-6'**), as well as those of cisplatin, carboplatin and oxaliplatin (Table 5). **5** and **5'** had not previously been tested in this panel of cell lines; the activity of **5** relative to **6** is consistent with previous cytotoxicity studies in that **6** is more active yet **5** is still very cytotoxic.[23] In most cell lines **6** is approx. 1.5-3 times more active than **5**, although **5** is more active than **6** against HT29 cells with an IC_{50} of 0.02 ± 0.01 μM. In contrast, **6** is approx. 15-60 times more active than **6'** in most cell lines; this reaffirms that while both the presence of methyl groups on the P_L and *SS*-dach as an A_L each improve cytotoxicity, the latter makes much more of a difference. The activity of **1-3** was lower than anticipated, with **1** being inactive in most lines and equivalent to cisplatin against HT29 cells. Complex **2** demonstrated notable activity in HT29 cells only, and was relatively inactive in most other cell lines. Complex **3** was more active than cisplatin in MIA cells, equivalent to cisplatin in A431 cells, and was comparable to **4'** against HT29, MCF-7, A2780 and BE2-C lines (Figure 7). The low cytotoxicity of **1-3** despite their high DNA affinity shows that DNA is not likely their target, or that the complexes are unable to reach nuclear DNA. It is clear that the improvement in cytotoxicity that 1,4-dach provides for kiteplatin over [Pt(*RR*-dach)Cl_2] is not transferrable to $[Pt(P_L)(A_L)]^{2+}$ complexes. Considering that 56MESS is known to disrupt cellular machinery through several methods unrelated to DNA,[18, 20, 39] and that the proposed mechanism of action of kiteplatin is the formation of DNA adducts that are harder to remove than those of cisplatin,[10] it is possible that the benefits of 1,4-dach over 1,2-dach only apply to the formation of covalent platinum-DNA adducts, which are not relevant for PPCs.

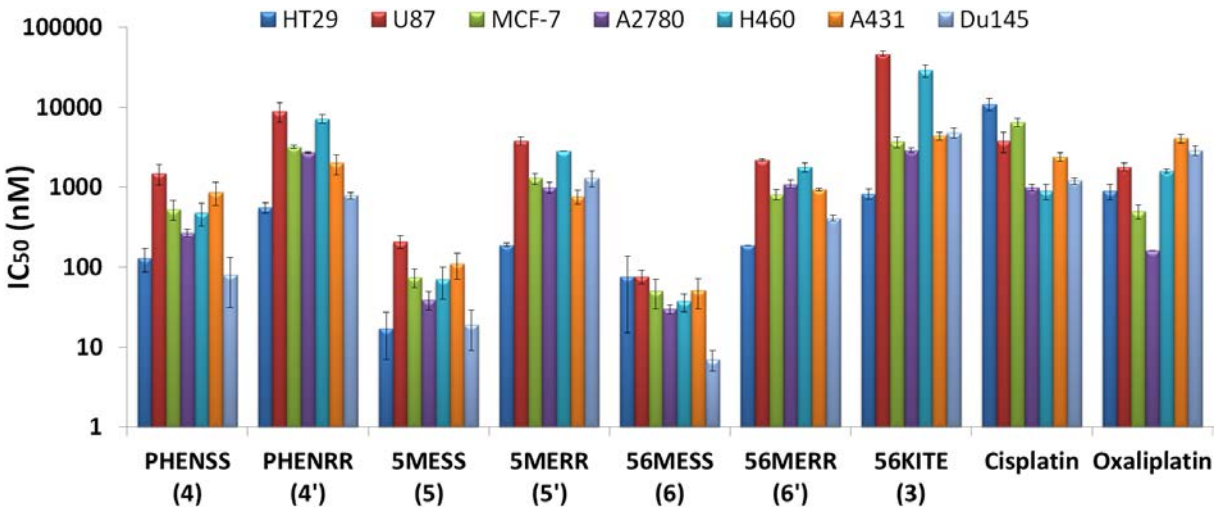

Figure 7. MTT assay-determined IC_{50} values of complexes **3-6**, **4'-6'**, cisplatin and oxaliplatin in several human cancer cell lines, expressed on a logarithmic scale in nanomolar with standard error. Complexes **1**, **2** and carboplatin were not included for clarity.

4. Conclusions

Three new platinum(II) derivatives of kiteplatin incorporating phen derivatives and 1,4-dach have been synthesised and characterised through several spectroscopic techniques. The CT-DNA binding of complexes **1-3** was assessed through ITC and compared to 1,2-dach analogues, revealing slightly higher DNA affinity for the former. The *in vitro* cytotoxicity of complexes **1-3** was found to be unexpectedly low in several human cell lines, with complex **3** demonstrating some results comparable with cisplatin. The results here indicate that the addition of 1,10-phenanthroline analogues to kiteplatin does not result in an improvement of anticancer activity and that DNA binding is not the primary mechanism of action of this type of complex.

Table 5. Summary of the *in vitro* cytotoxicity of complexes **1-3** and **1′-3′** in several cell lines, determined by the MTT assay and expressed as an IC_{50} value with standard error (1 sig. fig.). The activity of complexes **4-6** and **4'-6'**, as well as that of cisplatin, oxaliplatin and carboplatin is also included. IC_{50} is the concentration at which cell growth is inhibited by 50% over 72 h.

		IC_{50} (μM)										
	Complex	**HT29[a]**	**U87[a]**	**MCF-7**	**A2780**	**H460**	**A431**	**Du145**	**BE2-C**	**SJ-G2**	**MIA**	**MCF10A**
1	**PHENK**	10 ± 1	>50	>50	25 ± 3	>50	>50	>50	46 ± 4	>50	>50	>50
2	**5KITE**	2.1 ± 0.4	>50	14 ± 2	7 ± 1	>50	12 ± 2	43 ± 4	15.0 ± 0.3	30 ± 2	17 ± 2	50 ± 20
3	**56KITE**	0.8 ± 0.1	47 ± 3	3.7 ± 0.6	2.9 ± 0.2	29 ± 5	4.4 ± 0.5	4.8 ± 0.7	5.7 ± 0.7	17 ± 2	4.0 ± 0.4	5 ± 1
4	**PHENSS[a]**	0.13 ± 0.04	1.5 ± 0.4	0.5 ± 0.2	0.27 ± 0.03	0.5 ± 0.2	0.9 ± 0.3	0.08 ± 0.05	0.40 ± 0.05	0.45 ± 0.06	0.8 ± 0.7	0.16 ± 0.07
4'	**PHENRR[a]**	0.56 ± 0.08	8.9 ± 2.5	3.2 ± 0.2	2.70 ± 0.07	7.2 ± 0.9	2.0 ± 0.6	0.79 ± 0.08	3.8 ± 0.4	3.3 ± 0.3	2.7 ± 0.2	2.4 ± 0.3
5	**5MESS**	0.02 ± 0.01	0.21 ± 0.04	0.08 ± 0.02	0.04 ± 0.01	0.07 ± 0.03	0.11 ± 0.04	0.02 ± 0.01	0.3 ± 0.1	0.15 ± 0.03	0.10 ± 0.07	0.03 ± 0.01
5'	**5MERR**	0.19 ± 0.01	3.8 ± 0.4	1.3 ± 0.2	1.0 ± 0.2	2.8 ± 0.0	0.8 ± 0.2	1.3 ± 0.3	2.9 ± 0.2	2.9 ± 0.4	1.7 ± 0.2	1.6 ± 0.4
6	**56MESS[a]**	0.08 ± 0.06	0.08 ± 0.01	0.05 ± 0.02	0.030 ± 0.004	0.037 ± 0.009	0.05 ± 0.02	0.007 ± 0.002	0.10 ± 0.02	0.07 ± 0.02	0.015 ± 0.002	0.020 ± 0.005
6'	**56MERR[a]**	0.19 ± 0.00	2.2 ± 0.058	0.8 ± 0.1	1.1 ± 0.1	1.8 ± 0.2	0.93 ± 0.03	0.41 ± 0.04	2.3 ± 0.2	2.2 ± 0.2	0.45 ± 0.006	0.39 ± 0.01
	Cisplatin[a]	11 ± 2	4 ± 1	6.5 ± 0.8	1.0 ± 0.1	0.9 ± 0.2	2.4 ± 0.3	1.2 ± 0.1	1.9 ± 0.2	0.4 ± 0.1	8 ± 1	nd
	Oxaliplatin[a]	0.9 ± 0.2	1.8 ± 0.2	0.5 ± 0.1	0.16 ± 0.0	1.6 ± 0.1	4.1 ± 0.5	2.9 ± 0.4	0.9 ± 0.2	3 ± 1	0.9 ± 0.2	nd
	Carboplatin[a]	>50	>50	>50	9 ± 3	14 ± 1	24 ± 2	15 ± 1	19 ± 1	5.7 ± 0.2	>50	nd

[a] Reported in ref [21] and those within

Acknowledgments

We thank Western Sydney University for providing financial support through internal research grants. B.J.P. was supported by an Australian Postgraduate Award and a Western Sydney University Top-Up Award. Crystallographic data collection was undertaken on the MX1 beamline at Australian Synchrotron, Victoria, Australia.

References

1. Australian Institute of Health and Welfare and Australasian Association of Cancer Registries, *Cancer in Australia 2017*, Australian Institute of Health and Welfare, Canberra, 2017.
2. *Cancer Facts & Figures 2017*, American Cancer Society, Atlanta, Georgia, 2017.
3. N. J. Wheate, S. Walker, G. E. Craig and R. Oun, *Dalton Trans.*, 2010, **39**, 8113-8127.
4. M. G. Apps, E. H. Y. Choi and N. J. Wheate, *Endocr.-Relat. Cancer*, 2015, **22**, R219-R233.
5. B. H. Harper, F. Li, R. Beard, K. B. Garbutcheon-Singh, N. S. Ng and J. R. Aldrich-Wright, in *Supramolecular Systems in Biomedical Fields*, ed. H. J. Schneider, Royal Society of Chemistry, Cambridge, UK, 1st edn., 2013, ch. 9.
6. A.-M. Florea and D. Büsselberg, *Cancers*, 2011, **3**, 1351-1371.
7. J. D. Hoeschele, H. D. H. Showalter, A. J. Kraker, W. L. Elliott, B. J. Roberts and J. W. Kampf, *J. Med. Chem.*, 1994, **37**, 2630-2636.
8. N. Margiotta, C. Marzano, V. Gandin, D. Osella, M. Ravera, E. Gabano, J. A. Platts, E. Petruzzella, J. D. Hoeschele and G. Natile, *J. Med. Chem.*, 2012, **55**, 7182-7192.
9. J. Kasparkova, T. Suchankova, A. Halamikova, L. Zerzankova, O. Vrana, N. Margiotta, G. Natile and V. Brabec, *Biochem. Pharmacol.*, 2010, **79**, 552-564.
10. V. Brabec, J. Malina, N. Margiotta, G. Natile and J. Kasparkova, *Chem. Eur. J.*, 2012, **18**, 15439-15448.
11. E. Petruzzella, N. Margiotta, G. Natile and J. D. Hoeschele, *Dalton Trans.*, 2014, **43**, 12851-12859.
12. N. Margiotta, E. Petruzzella, J. A. Platts, S. T. Mutter, R. J. Deeth, R. Ranaldo, P. Papadia, P. A. Marzilli, L. G. Marzilli, J. D. Hoeschele and G. Natile, *Dalton Trans.*, 2015, **44**, 3544-3556.
13. S. Mutter, N. Margiotta, P. Papadia and J. Platts, *J. Biol. Inorg. Chem.*, 2015, **20**, 35-48.
14. J. Kasparkova, H. Kostrhunova, V. Novohradsky, J. Pracharova, A. Curci, N. Margiotta, G. Natile and V. Brabec, *Dalton Trans.*, 2017, **46**, 14139-14148.
15. N. Margiotta, S. Savino, C. Marzano, C. Pacifico, J. D. Hoeschele, V. Gandin and G. Natile, *J. Inorg. Biochem.*, 2016, **160**, 85-93.
16. N. Margiotta, S. Savino, N. Denora, C. Marzano, V. Laquintana, A. Cutrignelli, J. D. Hoeschele, V. Gandin and G. Natile, *Dalton Trans.*, 2016, **45**, 13070-13081.

17. A. Curci, N. Denora, R. M. Iacobazzi, N. Ditaranto, J. D. Hoeschele, N. Margiotta and G. Natile, *Inorg. Chim. Acta.*, 2017, In Press.
18. S. Wang, V. Higgins, J. Aldrich-Wright and M. Wu, *J. Chem. Biol.*, 2012, **5**, 51-61.
19. A. M. Krause-Heuer, R. Grünert, S. Kühne, M. Buczkowska, N. J. Wheate, D. D. Le Pevelen, L. R. Boag, D. M. Fisher, J. Kasparkova, J. Malina, P. J. Bednarski, V. Brabec and J. R. Aldrich-Wright, *J. Med. Chem.*, 2009, **52**, 5474-5484.
20. K. B. Garbutcheon-Singh, S. Myers, B. W. J. Harper, N. S. Ng, Q. Dong, C. Xie and J. R. Aldrich-Wright, *Metallomics*, 2013, **5**, 1061-1067.
21. B. J. Pages, J. Sakoff, J. Gilbert, A. Rodger, N. P. Chmel, N. C. Jones, S. M. Kelly, D. L. Ang and J. R. Aldrich-Wright, *Chem. Eur. J.*, 2016, **22**, 8943-8954.
22. R. Ranaldo, N. Margiotta, F. P. Intini, C. Pacifico and G. Natile, *Inorg. Chem.*, 2008, **47**, 2820-2830.
23. S. Kemp, N. J. Wheate, D. P. Buck, M. Nikac, J. G. Collins and J. R. Aldrich-Wright, *J. Inorg. Biochem.*, 2007, **101**, 1049-1058.
24. T. M. McPhillips, S. E. McPhillips, H. J. Chiu, A. E. Cohen, A. M. Deacon, P. J. Ellis, E. Garman, A. Gonzalez, N. K. Sauter, R. P. Phizackerley, S. M. Soltis and P. Kuhn, *J. Synchrotron Radiat.*, 2002, **9**, 401-406.
25. W. Kabsch, *J. Appl. Crystallogr.*, 1993, **26**, 795-800.
26. SADABS: Empirical Absorption and Correction Software, University of Göttingen, 1998.
27. G. M. Sheldrick, *Acta Crystallogr., Sect. C: Cryst. Struct. Commun.*, 2015, **71**, 3-8.
28. G. M. Sheldrick, SHELXT-2014, University of Göttingen, 2014.
29. G. M. Sheldrick, SHELXL-2014, University of Göttingen, 2014.
30. O. V. Dolomanov, L. J. Bourhis, R. J. Gildea, J. A. K. Howard and H. Puschmann, *J. Appl. Crystallogr.*, 2009, **42**, 339-341.
31. B. J. Pages, J. Sakoff, J. Gilbert, Y. Zhang, F. Li, D. Preston, J. D. Crowley and J. R. Aldrich-Wright, *J. Inorg. Biochem.*, 2016, **165**, 92-99.
32. B. J. Pages, F. Li, P. Wormell, D. L. Ang, J. K. Clegg, C. J. Kepert, L. K. Spare, S. Danchaiwijit and J. R. Aldrich-Wright, *Dalton Trans.*, 2014, **43**, 15566-15575.
33. K. B. Garbutcheon-Singh, P. Leverett, S. Myers and J. R. Aldrich-Wright, *Dalton Trans.*, 2013, **42**, 918-926.
34. S. Kemp, N. J. Wheate, M. J. Pisani and J. R. Aldrich-Wright, *J. Med. Chem.*, 2008, **51**, 2787-2794.
35. B. M. Still, P. G. A. Kumar, J. R. Aldrich-Wright and W. S. Price, *Chem. Soc. Rev.*, 2007, **36**, 665-686.
36. A. R. Khokhar, S. Shamsuddin and Q. Xu, *Inorg. Chim. Acta.*, 1994, **219**, 193-197.
37. L. M. Salonen, M. Ellermann and F. Diederich, *Angew. Chem., Int. Ed.*, 2011, **50**, 4808-4842.
38. B. N. Anila, N. M. K. Muraleedharan, J. Sreedharan and V. P. Sylas, *Asian J. Chem.*, 2017, **29**, 691-702.
39. S. Wang, M. J. Wu, V. J. Higgins and J. R. Aldrich-Wright, *Metallomics*, 2012, **4**, 950-959.